Solar-Thermal Hybridization of Advanced Zero Emissions Power Plants

by

Ragheb Mohamad Fawaz El Khaja

Submitted to the
Department of Mechanical Engineering
in Partial Fulfillment of the Requirements for the Degree of

Bachelor of Science in Mechanical Engineering

at the

Massachusetts Institute of Technology

June 2012

Signature of Author .....
Department of Mechanical Engineering
May 24, 2012

Certified by .....
Alexander Mitsos
Rockwell International Assistant Professor
Thesis Supervisor

Accepted by .....
John H. Lienhard V
Samuel C. Collins Professor of Mechanical Engineering
Undergraduate Officer

Solar-Thermal Hybridization of Advanced Zero Emissions Power Plants

by

Ragheb Mohamed Fawaz El Khaja

Submitted to the Department of Mechanical Engineering on
May 24, 2012 in partial fulfillment of the requirements for the
Degree of Bachelor of Science in Mechanical Engineering

ABSTRACT

Carbon Dioxide emissions from power production are believed to have significant contributions to the greenhouse effect and global warming. Alternative energy resources, such as solar radiation, may help abate emissions but suffer from high costs of power production and temporal variations. On the other hand, Carbon Capture and Sequestration allows the continued use of fossil fuels without the CO_2 emissions but it comes at an energetic penalty. The Advanced Zero Emissions Plant (AZEP) minimizes this energy loss by making use of Ion Transport Membrane (ITM)-based oxy-combustion to reduce the cost of carbon dioxide separation. This work seeks to assess if there are any thermodynamic gains from hybridizing solar-thermal energy with AZEP. The particular focus is hybridizing of the bottoming cycle with supplemental solar heating. A simple model of parabolic solar trough was used to hybridize a model of the AZEP cycle in ASPEN Plus®. Two cycle configurations are studied: the first uses solar parabolic troughs to indirectly vaporize high pressure steam through Therminol and the second uses parabolic troughs to directly preheat the high pressure water stream prior to vaporization.

Simulations of the solar vaporizer hybrid by varying the total area of collectors (holding fuel input constant) show an increase of net electric output from 439MW for the non-hybridized AZEP to 533MW with an input solar share of 38.8%. The incremental solar efficiency is found to be around 16% for solar shares of input ranging from 5% to 38.8%. Moreover, simulations of variable solar insolation for collector area of 550,000 m^2, show that incremental solar efficiency increased with solar insolation reaching a plateau around 17%. Simulations of the direct solar preheater, show a net electric output of 501.3 MW for a solar share of 35%, (an incremental solar efficiency of 13.73%). The power generation and hence incremental efficiency is lower than in hybridization with steam vaporization with the same input solar share. Synergy analysis for the steam vaporization hybrid indicates no thermodynamic gains from hybridization.

Thesis Supervisor: Alexander Mitsos
Title: Rockwell International Assistant Professor

ACKNOWLEDGEMENTS

This thesis would not have been possible without the support and contribution of many individuals; I am eternally grateful.

To my advisor, Professor Alexander Mitsos, for his guidance throughout the project. Our discussions taught me how to pose the right questions and helped me develop my skills as an engineer.You were a source of motivation and a strong driving force forward!

To Nick Mancini whose work inspired this project. Nick's models of Ion Transport Membranes and the AZEP cycle were central for this investigation and I am grateful for being allowed to use them.

To Elysia Sheu, for conceptual discussions and technical guidance. Elysia's development of a model of parabolic troughs greatly facilitated this work and for that I am very thankful.

To my Labmates - Hussam and Gina, for their support and guidance in the technical aspects of this work. Surekha, for her valuable feedback and discussions on this thesis. To Tawfiq, Dan, Enrique, Jun and Abishek, it was a pleasure being your labmate and I will miss you all.

To my family, for always encouraging me to pursue my dreams. To my Mother, Maha, for being my inspiration, supporting me every step of the way and loving me unconditionally. To my Father, Fawaz, for sparking my interest in science, teaching me to question everything and believing in me. To my sister, Aya, for pushing me forward and inspiring me to never give up. I love you all dearly.

To Samer, for being a dear friend and always standing by my side. Thank you for being there at every bump in the road: cheering me on and making me laugh.

"If you can dream - and not make dreams your master;

If you can think – and not make thoughts your aim;"

-Rudyrad Kipling

Table of Contents

List of Figures

List of Tables

1. Introduction

Anthropogenic carbon dioxide emissions are widely considered to be a "very likely" cause of global warming [1]. Electric power generation is a major source of carbon dioxide emissions. As the world population and economy continue to grow, the demand for electricity is expected to continue to increase. Fossil fuels, the primary source of energy for electricity generation, have the drawbacks of being emissions heavy, unsustainable and politically restricting [2]. Nonetheless, fossil fuels continue to be a valuable resource due to their high energy density and reliability for continuous power generation. Much research has gone into investigating ways of reducing carbon dioxide emissions from electric power generation. Alternative energy resources, such as solar energy, hold promise as future replacements of fossil fuels. Solar energy is an attractive option due to the large amount of insolation available from the sun. There are major limitations to solar energy including: the need for large collector areas (leading to high costs) and the temporal variability of supply (necessitating energy storage and/or backup fossil fuel generators). Hybrid solar-fossil fuel power generation, where solar energy and fossil fuel are used simultaneously, offers a method to alleviate these high costs and intermittency problems. Alternatively, carbon capture and sequestration (CCS) can allow the use of fossil fuels without the associated CO_2 emissions, helping bridge the transition to renewable energy resources. This reduction in emissions, however, comes at a high economic and thermodynamic cost [3]. This thermodynamic cost of CCS implies that efficiency gains in a power plant that employs CCS may be doubly rewarded: carbon emissions are reduced, which reduces the power requirement of CCS, which in turn reduces carbon emissions, etc. [4] Therefore, power plants with CCS may be prime candidates for solar-thermal hybridization. This work investigates the potential benefits from solar-thermal hybridization of zero-emissions power cycles with ITM-based oxy-combustion carbon capture and sequestration.

Concentrated Solar-Thermal Power

Solar radiation is a major source of renewable energy. Solar-thermal power generation converts solar radiation to electrical power. A concentrated solar receiver is used to heat a working fluid (directly or via a heat transfer fluid), which is then used to drive the power cycle. Receiver technologies have varied operating conditions, technological maturity and typical solar-to-electric efficiencies. Concentrated solar receiver-collector systems include:

- Parabolic/Linear Frensel Trough Systems
- Central Receiver Systems (Heliostat + Receiving Tower)
- Solar Dish Systems

The heat from the receiver can be used either to replace combustors in traditional power plants, or as a supplementary heat source in hybrid solar-fossil fuel plants.

Parabolic Trough

Parabolic trough technology uses a single axis tracking parabolic mirror to focus sunlight on a receiver pipe at the focal point [5]. Parabolic troughs are used to provide heat to a power cycle either directly by heating the working fluid, or indirectly through a heat transfer fluid (usually mineral or synthetic thermal oil), which is used to heat the working fluid. It is the most mature solar-thermal technology. Therefore, there is a low technology development risk, which makes parabolic trough a good fit for solar-fossil fuel hybridization. Parabolic troughs have been

demonstrated to operate at temperatures up to 390°C at a peak solar-to-electric first law efficiency of 20% [10]. In the Mojave Desert in California, parabolic troughs are used to power 9 power plants in the Solar Electric Generating System (SEGS) with a backup natural gas utilization capacity for dispatchablity. These power plants have been in operation for over 25 years, producing a total of 354MW of California's electric power, which shows the technical maturity of solar-thermal technology [10].

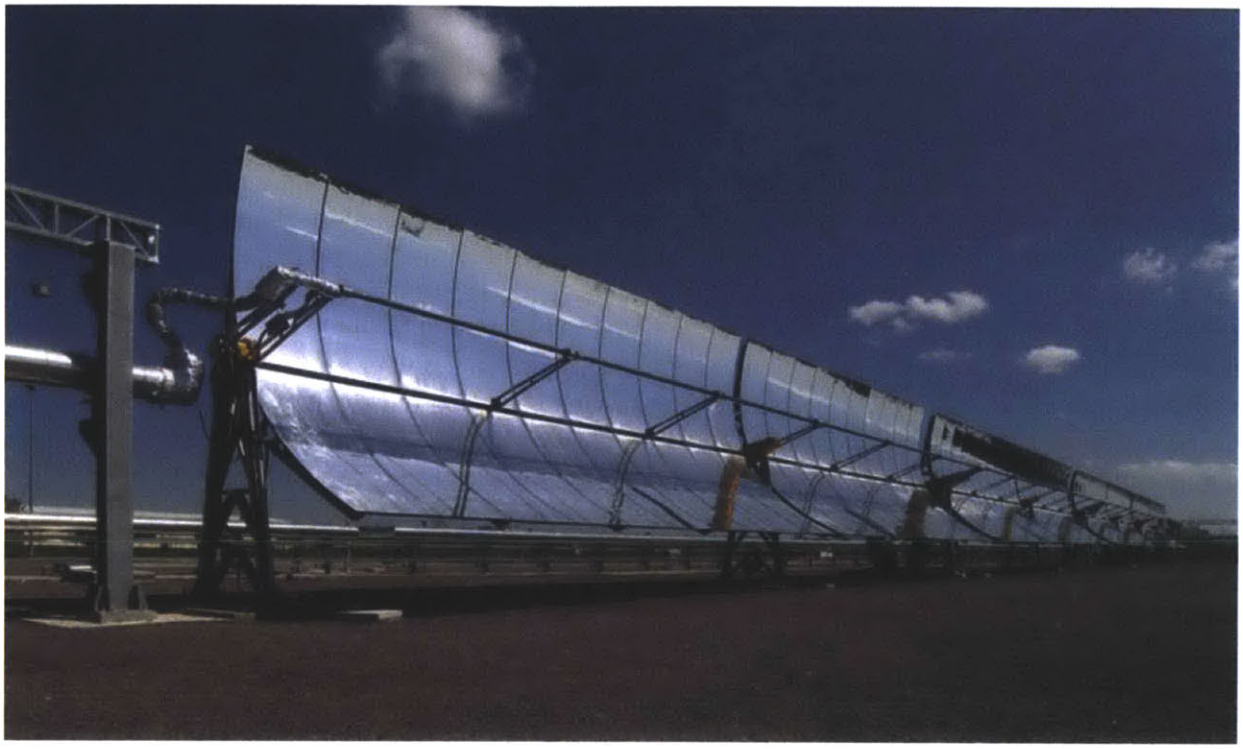

Figure 1. Parabolic Trough Solar Collector Assembly (Source: Archimede Solar Energy)

Hybrid Solar-Fossil Fuel Power Generation

Hybridization of solar-thermal power generation with fossil fuels allows the offset of high cost and intermittency problems typical in solar power generation. Hybridization here refers to power plants that use both solar and fossil fuel energy simultaneously (i.e. not plants that use combustors as a source of backup energy for dispatchable generation) and the focus is on combined cycles with carbon capture. There are several options for the integration of solar-thermal energy with combined cycles. Solar-thermal energy can be used to preheat compressed air to moderate temperatures prior to combustion. This integration scheme has high efficiency but requires relatively immature technology to achieve the high operating temperatures [7]. Alternatively, solar-thermal energy can provide supplemental energy to heat recovery steam generation (HRSG). This integration model does not require as high of operating temperature, allowing the use of mature parabolic trough technology. The supplementary solar energy to the HRSG can be used either to preheat water feed, for steam generation (vaporization), or both.

Carbon Capture and Sequestration

Carbon capture and sequestration (CCS) is a process that allows continued use of fossil fuels for power generation by the separation of CO_2 from the exhaust and its compression to high pressures for storage in deep geological formations or ocean masses. CCS introduces large efficiency and cost penalties. CO_2 separation can be achieved by different strategies:

- Post-combustion treatment of flue gases to separate CO_2, including using adsorption, selective membranes, distillation or other techniques.
- Pre-combustion treatment of the fossil fuels such as the production of syngas from coal gasification and adsorption of produced CO_2.
- Oxyfuel combustion, where the fossil fuel is combusted in the absence of nitrogen, yielding only CO_2 and steam allowing separation by simple condensation [8].

Oxyfuel combustion is promising due to its relatively low CO_2 separation penalty but it suffers from a cost/energy penalty for the production of pure oxygen. Conventionally, large-scale oxygen production employs cryogenic techniques, multi-stage distillation processes at low temperature which require a large amount of electrical energy, resulting in first law efficiencies loss of up to 8.5 percent points compared to NGCC without CCS [9, 10, 11].

An alternative technique for oxygen separation is Ion Transport Membrane (ITM), a mixed-conducting (ionic and electronic) ceramic membrane to separate oxygen from air. ITMs rely on the difference in chemical potential of O_2 as the driving force of separation [12] and typically operate at high temperatures (>1000K). Since the separation is passive, the primary mode of energy loss in ITMs is drop in pressure and in some cases operational constraints. Therefore, ITMs have lower energy penalty than cryogenic techniques. Commercial scale ITM O_2 modules were produced by Air Products that have 35% lower capital cost and up to 60% lower energy penalty when compared to cryogenic air separation, which shows the promise of this novel technique [13].

Advanced Zero Emissions Power Plants

The Advanced Zero Emissions Plant (AZEP) is a conceptual design of a power plant that incorporates CCS with ITM-based oxy-combustion to a conventional combined cycle gas turbine. By employing ITM-based oxy-combustion, AZEP decreases the energy penalty of oxygen separation and CO_2 capture (compared with conventional CCS) [14]. There are alternatives for the AZEP cycle which utilize an afterburner to increase efficiency at the cost of partial emissions, but the focus herein is the AZEP with complete capture. Thermal efficiencies reported for AZEP range from 48.9% to 52.5% [4, 14, 15].

2. Project Context, Objectives and General Approach

This project analyzes the potential benefit from the solar-thermal hybridization of power plants with CCS based on ITM oxy-combustion. This potential benefit was proposed by Mancini [4].

Project Objectives

The primary motivation of this project is to assess the potential for thermodynamic benefits from hybridizing AZEP with solar-thermal energy. Specifically:

-To study an innovative plant concept that hybridizes solar energy and ITM oxy-combustion based CCS.

-To compare the thermodynamic performance of different modes of hybridization.

-To assess how the hybrid system responds to inherent fluctuations in solar insolation.

-To investigate the thermodynamic gains from hybridization (synergy) compared to a meaningful linear combination of solar-only plant and AZEP.

-To identify potential improvements in the hybrid design for future research.

General Approach

To achieve the above listed objectives, simulations of AZEP in ASPEN Plus® were hybridized with solar parabolic troughs.

The following section (**Chapter 3**) describes the models used in the simulation: an ASPEN Plus® model of AZEP, an intermediate-fidelity model of the ITM in JACOBIAN and a simple 1-D model of parabolic troughs in ASPEN Custom Modeler®. Afterwards, the performance and design metrics used in this work are detailed (**Chapter 4**).

This is followed by a simulation of a hybridized AZEP cycle with solar parabolic trough providing the heat of vaporization for the high pressure steam generation indirectly through an intermediate heat transfer fluid (**Chapter 5**), varying solar share while assuming constant solar insolation and angle of incidence. Subsequently, the cycles thermodynamic performance for a fixed area of solar collectors with varying levels of solar insolation is analyzed (**Chapter 6**).

An alternative integration scheme, where solar parabolic troughs are used directly to preheat the high pressure water stream prior to vaporization is simulated and its performance analyzed in **Chapter 7.**

An analysis of the potential thermodynamic synergy from hybridization (as compared to a linear combination of solar-only and AZEP cycles) is performed in **Chapter 8**.

Finally, a discussion of the results of these simulations and potential future work is laid out in **Chapter 9**.

3. Models Description

AZEP Cycle

The AZEP cycle simulation used in this work was developed in ASPEN Plus® by previous work by Mancini and Mitsos [4, 16, 17]. ASPEN Plus® is a modular process modeling tool with pre-defined unit model operations that can be used for power cycle flowsheet simulation. The AZEP cycle can be divided into three subunits: a Brayton-Like cycle with an integrated JACOBIAN ITM model (**Figure 2**), a Triple Pressure Heat Recovery Steam Generator (HRSG) (**Figure 3**) and a Carbon Compression and Purification unit (**Figure 4**).

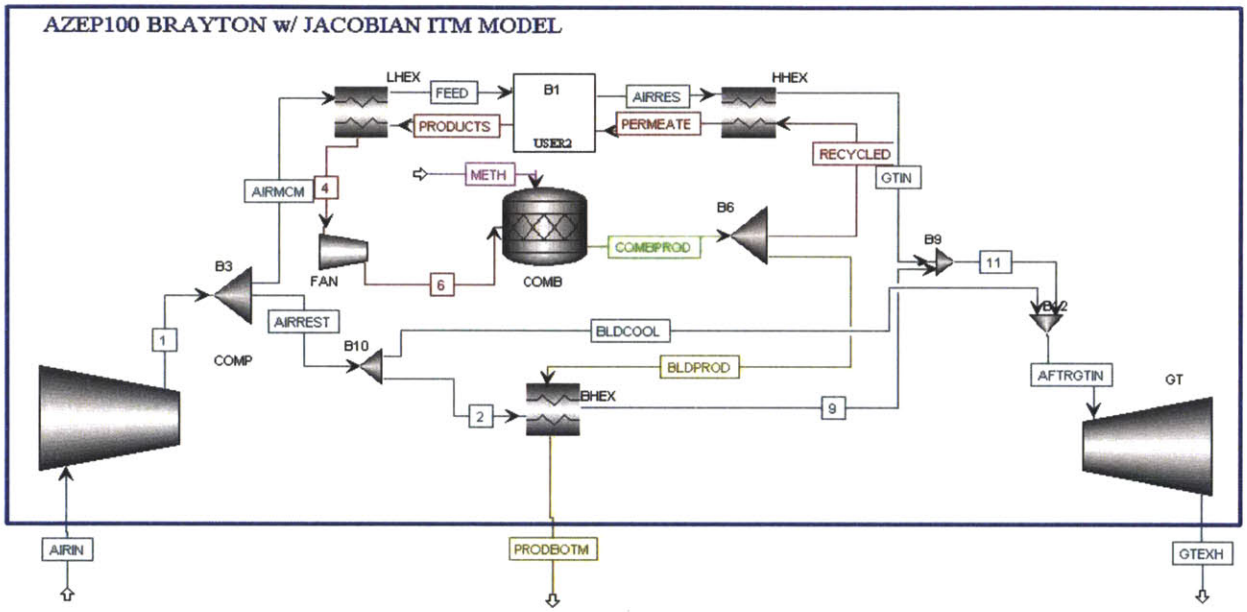

Figure 2. ASPEN Plus® Model – Brayton-Like Topping Cycle [17].

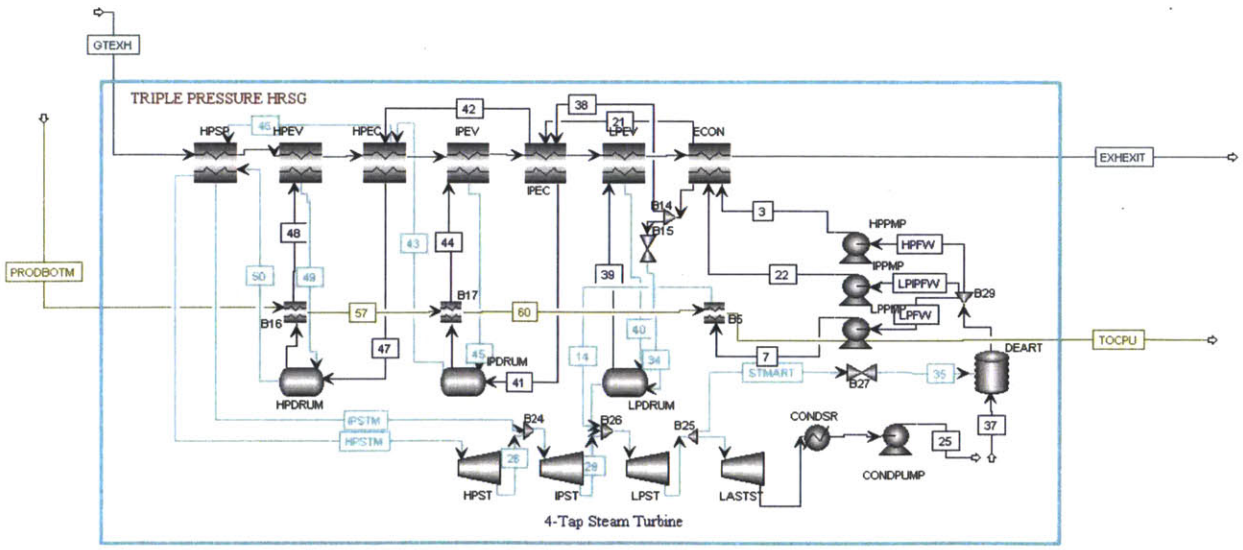

Figure 3. ASPEN Plus® Model - Triple Pressure Heat Recovery Steam Generator [17].

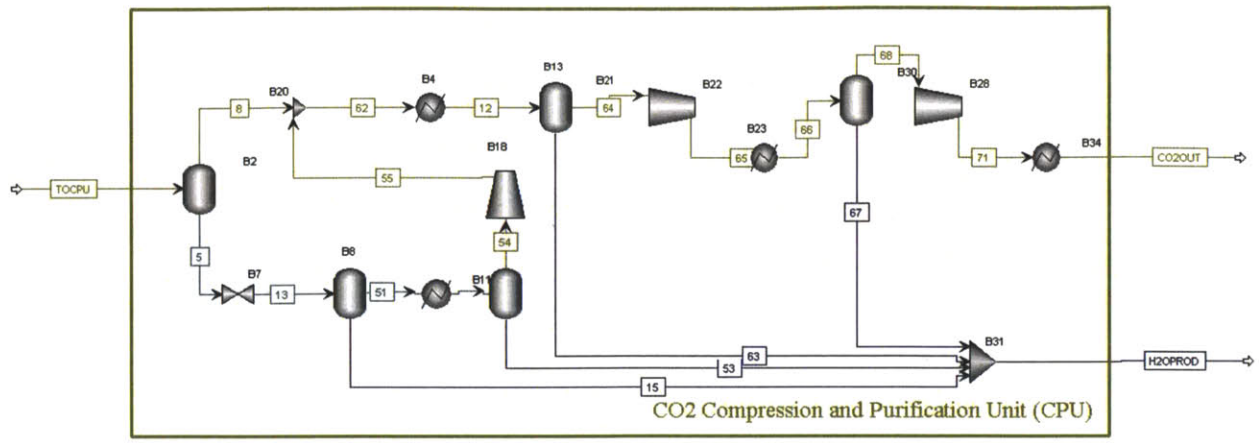

Figure 4. ASPEN Plus® Model - CO_2 Compression and Purification Unit [17].

The topping Brayton-like cycle contains a separation-only ITM and a methane oxy-combustor. Air is compressed and fed into the ITM, where the oxygen is driven to a recycled permeate stream of CO_2 and steam from the combustion products. A system of heat exchangers (LHEX, HHEX) is used to transfer heat from the recycled combustion products to the air feed. The combustion product is used to heat a fraction of the compressed air. The heated compressed air is combined with oxygen-deprived air out of the ITM to drive a gas turbine; a blade cooling stream is used. The proportion of these streams is designed so that the turbine inlet temperature is maintained constant. The combustion product and the turbine exhaust are then fed into the HRSG bottoming cycle.

The triple pressure HRSG uses the residual heat in the turbine exhaust to drive steam generation for three steam streams at pressures 100bar, 25bar and 5bar. The triple pressure design decreases entropy generation in the heat exchangers by reducing the temperature gap at vaporization. The turbine exhaust is used to heat and vaporize the different pressure streams and superheat the high and intermediate pressure streams. The combustion product stream provides supplemental heat for the vaporization of the three steam streams and then sent to the CO_2 compression and purification unit. The steam streams are then used for power generation four steam turbines cascade. The simulation of this cycle is described in detail in **Appendix A**.

The CO_2 compression and purification unit takes in the combustion product after it is cooled in the HRSG, condenses steam out and compresses the residual CO_2. The incoming stream consists of only CO_2 and H_2O since methane is combusted with the ITM products (O_2, CO_2 and H_2O) and not air. Therefore, step-wise condensation of water and compression of CO_2 is sufficient for CCS.

ITM Model

An intermediate-fidelity model was developed in JACOBIAN by previous work that is detailed enough to capture the physics of the ITM without excessive computational expense. This is ideal for the design of oxy-combustion power cycles. The model relies on basic principles, in addition to semi-empirical relations, to characterize the performance of ITMs [4,

16]. The JACOBIAN model is linked to power cycles in ASPEN Plus® via Excel by using the User2 module in ASPEN Plus®.

The model developed can be used for both reactive ITMs and separation-only ITMs. The analysis by Mancini and Mitsos found that the potential benefits from reactive ITMs appear to be outweighed by the restraints of meeting operational constraints [17]. Therefore, this work focuses on separation-only ITMs.

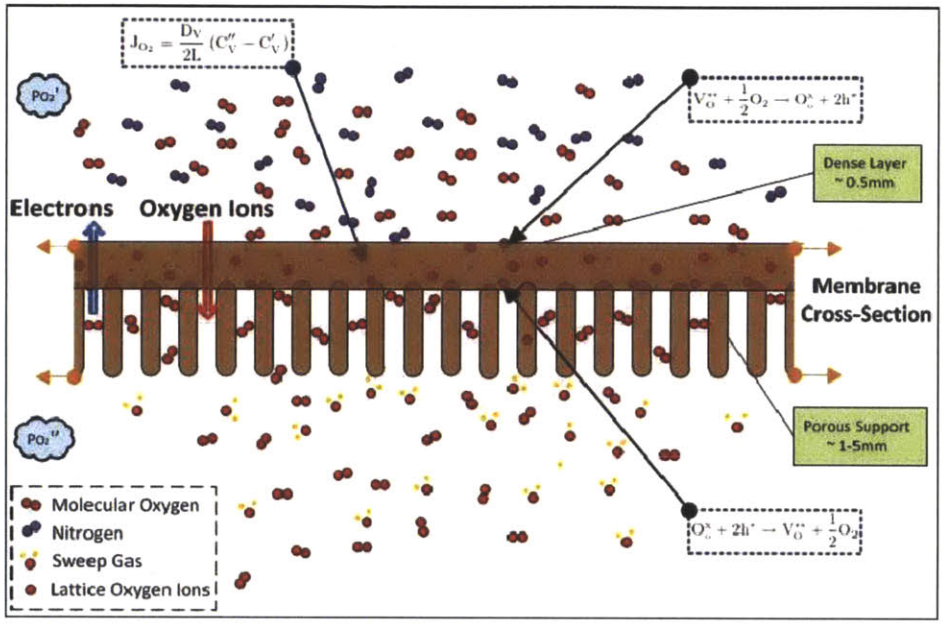

Figure 5. Ion Transport Membrane Air Separation Process [4]

Parabolic Trough Model

A model of parabolic troughs was implemented in ASPEN Custom Modeler® by Elysia Sheu at Mitsos Lab at MIT. This model is based on the work described in NREL Technical Report "Heat Transfer Analysis and Modeling of a Parabolic Trough Solar Receiver Implemented in Engineering Equation Solver" [18].

The receiver is modeled as a steel pipe covered with a glass cover with vacuum in between.

The optical efficiency of the receiver, η_0 is modeled as:

$$\eta_0 = e1\ e2\ e3\ e4\ e5\ e6\ K\ \rho_{cl}\ \tau$$

Where τ is the transmittance of the glass cover, ρ_{cl} is the clean mirror reflectance, K is the incident angle modifier and $e1$-6 are optical parameters as defined in **TABLE 1** below.

TABLE 1. Optical Parameter Values Assumed in Parabolic Trough Model.

Parameter	Description	Value
$e1$	Shadowing Parameter	0.974
$e2$	Tracking Error	0.994
$e3$	Geometry Error	0.98
$e4$	Dirt on Mirror Parameter	Reflectivity of clean mirror/ ρ_{cl}
$e5$	Dirt on Receiver Parameter	$\frac{1+e4}{2}$
$e6$	Random Error	0.96

K, the incident angle modifier, can be modeled as a function of θ, the incidence angle, by:

$$K = \cos(\theta) + 0.000884\theta - 0.0000536 9\theta^2$$

The amount of energy absorbed by the pipe Q_{abs} is found using:

$$Q_{abs} = q\ A\ \alpha\ \eta_0$$

Where q is solar insolation, A is total area of collector, α is the absorptance of the pipe and η_0 is the optical efficiency of the receiver.

The trough system is modeled as a one dimensional resistance network and the convective resistances are estimated using Nusselt number correlations.

4. Performance and Design Metrics

The following is a description of the performance metrics used in this study to analyze the results of simulations of solar-thermal hybridized cycles [5].

Solar Share

Solar Share of Input is defined as the portion of incoming energy provided by solar energy. It is calculated as follows:

$$X_{S,I} = \frac{\dot{Q}_{solar}}{\dot{Q}_{solar} + \dot{Q}_{fuel}}$$

Where $\dot{Q}_{solar}$ is the incoming energy rate from solar, defined as $\dot{Q}_{solar} = A \cdot \dot{q}$, where A is total collector area of parabolic troughs (in m^2), $\dot{q}$ is solar insolation (in W/m^2), and $\dot{Q}_{fuel}$ is the heating rate input from fuel defined as: $\dot{Q}_{fuel} = \dot{m} \cdot LHV$, where $\dot{m}$ is the fuel mass flow rate and LHV is the fuel lower heating value per unit mass.

Solar Share of Output is defined as the portion of the net produced work that is accounted for by solar energy. It is calculated as follows:

$$X_{S,O} = \frac{\dot{W} - \eta_{ref}\,\dot{Q}_{fuel}}{\dot{W}}$$

Where η_{ref} is the reference first law efficiency of the non-hybridized cycle. Herein the AZEP efficiency as calculated by Mancini and Mitsos [17] is used for η_{ref}.

The net electrical power, $\dot{W}$, is calculated as the power out of the gas turbine and steam turbines minus the power consumption of the air compressor, air fan, water pumps in the bottoming cycle, Therminol pump and CO_2 compressors.

Efficiencies

The First Law Efficiency for a hybrid solar power cycle is defined as:

$$\eta_I = \frac{\dot{W}}{\dot{Q}_{solar} + \dot{Q}_{fuel}}$$

Since typically solar to electric efficiency for solar plants is lower than fuel to electricity efficiency of fossil fuel plants, first law efficiency is typically decreasing with solar share.

The Second Law Efficiency for a hybrid solar power cycle is defined as:

$$\eta_{II} = \frac{\dot{W}}{\dot{E}_{solar} + \dot{E}_{fuel}}$$

Where $\dot{E}_{fuel}$ is the exergy rate for fuel and $\dot{E}_{solar}$ is the exergy rate for solar input, estimated as:

$$\dot{E}_{solar} = \dot{Q}_{solar}\left(1 - \frac{T_0}{T_i}\right)$$

Where T_0 is the ambient temperature (298K) and T_i is the internal temperature of the sun (~5800K).

The Net Incremental Solar Efficiency is a measure of efficiency of the solar portion of the hybrid power plant, defined as

$$\eta_{net-incr-solar} = \frac{\dot{W} - \eta_{ref}\dot{Q}_{fuel}}{\dot{Q}_{solar}}$$

5. Solar-Thermal Indirect High Pressure Steam Vaporization

Solar energy can be used to evaporate steam in the bottoming cycle of the AZEP. Parabolic troughs are used to vaporize steam indirectly through a heat transfer fluid. This section presents a simulation of this mode of solar-thermal hybridization.

Design Description

The bottoming cycle in AZEP plants uses heat from the turbine exhaust to heat and vaporize three streams of water flow at pressures 100bar, 25bar and 5bar. Vaporization presents a temperature mismatch between the exhaust flow and the steam flow which introduces entropy generation. Therefore, there may be benefit from using solar heat for vaporization, allowing closer matching of the temperature profiles. To investigate this, an ASPEN Plus® model of AZEP was hybridized by the introduction of parabolic troughs to heat an intermediate heat transfer fluid, Therminol VP-1, which is used to vaporize high pressure steam in the bottoming cycle in a counter-current heat exchanger. This proposed design of the bottoming cycle is shown in the following schematic (**Figure 6**).

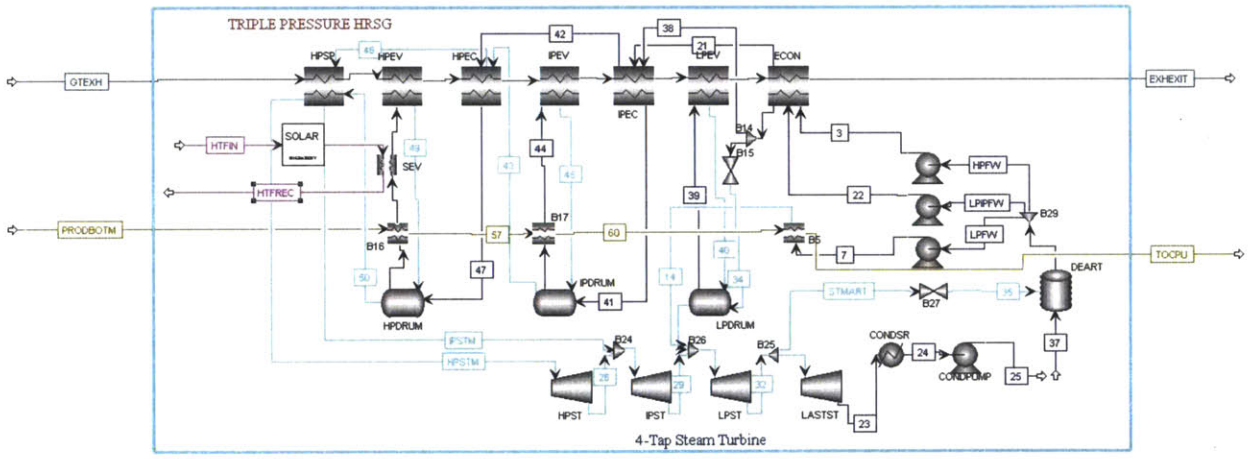

Figure 6. Schematic of AZEP Bottoming Cycle with Indirect Solar Vaporization of High Pressure Steam.

Simulation Description

The solar parabolic trough field consists of 50 parabolic troughs running in parallel to heat Therminol VP-1 (in the liquid phase). Therminol flow rate was maintained constant while the total area and length of the parabolic troughs were varied to obtain desired solar shares. The area and length parameters were varied, to reach target vapor fractions out of the solar vaporizers. This is a simulation of the solar-hybridized bottoming cycle at an instant in time, so it assumes constant solar insolation and angle of incidence. Modifications to the bottoming cycle do not have an effect on the topping cycle, therefore, the output streams of the topping cycle (Gas Turbine Exhaust and Air Combustion Products) are assumed to be unaffected by hybridization and taken as fixed inputs.

The properties and input parameters used for the solar parabolic troughs are shown in **TABLE 2** below.

TABLE 2. Input Parameters and Properties Used in Simulation of Solar Parabolic Troughs for Therminol Heating.

Number of Parallel Troughs	50
Solar Insolation	500 W/m^2
Incident Angle	45°
Therminol VP-1 Flow Rate	0.2 kmol/s/trough
Therminol Input Pressure	20 bar
Therminol Input Temperature	590.1 K
Solar Heat Exchanger Therminol Output Temperature (Recycled)	590.1 K
Trough Pipe Length	Receiver Area/ 5.5

The Therminol recycle temperature was chosen for a pinch ΔT in the heat exchanger of 6°C. The Therminol input pressure was chosen so as to insure that the heat transfer fluid is remains in liquid phase throughout the parabolic troughs.

Simulation Results

This section presents the major findings of the simulation of this hybridization scheme. A summary of the energetic results is presented in the TABLE below:

TABLE 3. Results of Simulation of AZEP Hybridized with Indirect Solar-Thermal Vaporizer in Bottoming Cycle. Light Grey indicates the non-hybridized AZEP cycle for reference [4].

Area of Solar Troughs (m^2)	0	98,000	323,000	526,000	764,000	1,160,000
Solar Heat Input (MW)	0	49.2	161.6	262.9	382.1	579.8
Solar Share of Input (%)	0	5	15	22.3	29.5	38.8
Net Electricity Produced (MW)	438.7	446.7	465.0	481.4	502.0	532.7
First Law Efficiency (%)	47.93	46.31	43.18	40.86	38.70	35.63
Second Law Efficiency (%)	46.08	44.73	42.08	40.07	38.20	35.47
Solar Share of Output (%)	0	1.8	5.7	8.9	12.6	17.7
Incremental Solar Efficiency (%)	N/A	16.27	16.32	16.26	16.59	16.21

The Net Electricity Produced increased as the total area of solar troughs increased (holding fuel input constant), i.e. the incremental solar efficiency was positive. As the solar share increased, first law efficiency decreased. This is consistent with expectations because solar-to-electric efficiency is typically significantly lower than fuel-to-electricity efficiency, so a hybrid is expected to have a lower thermal efficiency than a fuel only plant. Similarly, second law efficiency was found to decrease with solar share of input. Net electric output was plotted as a function of collector area, shown in **Figure 7.** Since solar insolation and angle of incidence are held constant, collector area is equivalent to solar heating rate. It can be seen that as area of the collectors increases, the net electric output also increases almost linearly, consistent with a constant incremental solar efficiency. Interestingly, incremental solar efficiency appeared practically unaffected by solar share and remained around 16%. This unexpected result prompts further investigation as the relationship between solar share and incremental solar efficiency is a critical one for cost-benefit analysis on solar hybridization.

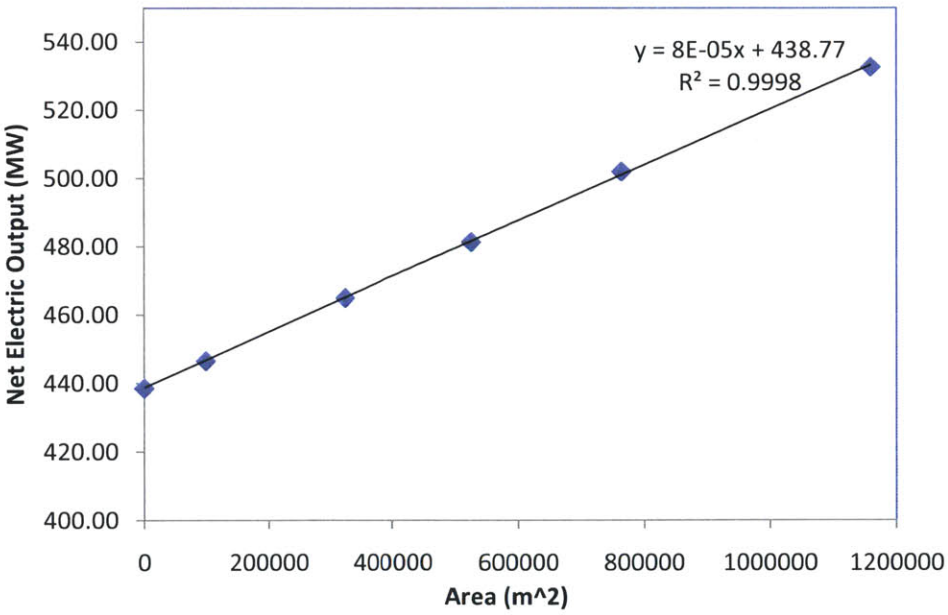

Figure 7. Plot of Net Electric Output as a Function of Total Collector Area in High P Vaporizer Hybridized AZEP plants. Insolation and angle of incidence are set at values of 500W/m^2 and 45°, respectively, while the total collector area of the parabolic troughs is varied in the simulation.

The solar parabolic troughs increase electric production by allowing more steam to flow through the HRSG. Therefore, investigating the effect of this hybridization scheme on the temperature profile of the exhaust may provide valuable insights. A pinch diagram was plotted for the non-hybridized AZEP bottoming cycle along with a sample hybridized cycle (solar share 15%) in **Figure 8**.

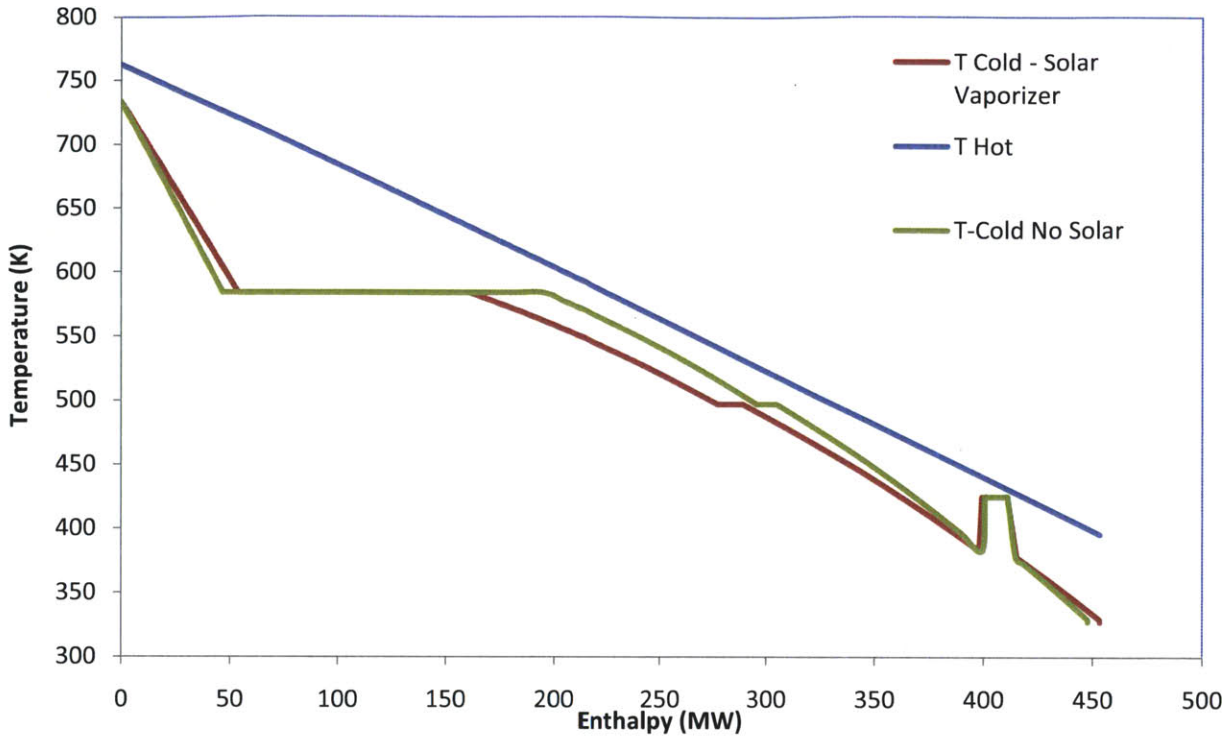

Figure 8. Pinch Diagram for Gas Turbine Exhaust Heat Exchangers in Bottoming Cycle for a non-hybridized AZEP cycle (green) and a high pressure steam solar vaporizer hybridized cycle with solar share 15% (red).

From the pinch diagram above, it is clear that this hybridization scheme increases the temperature mismatch in the heat exchanger increasing entropy generation. It is important to note that this is not an optimized flowchart and there may be ways to improve the temperature profile match and increase efficiency. The solar vaporizer inputs heat at 584.1 K (boiling temperature at pressure of 100bar), which allows more steam flow in the high pressure stream. As a consequence, more heat is needed to preheat the high pressure water flow to liquid saturation. Therefore, high P vaporization occurs when the exhaust at a higher temperature (compared to no-solar case) which leads to the increased temperature profile mismatch. The temperature mismatch might be less if solar heat is used for vaporization of low pressure steam instead of high pressure steam. Further investigation should go into the choice of where to implement solar vaporization.

The increased steam flow rate through the economizer leads to higher heat extraction from the gas turbine exhaust and lower exit exhaust residual enthalpy- as shown in **Figure 9**. This increase in exhaust enthalpy extraction may compensate for the entropy generation due to the worsening in temperature profile mismatch.

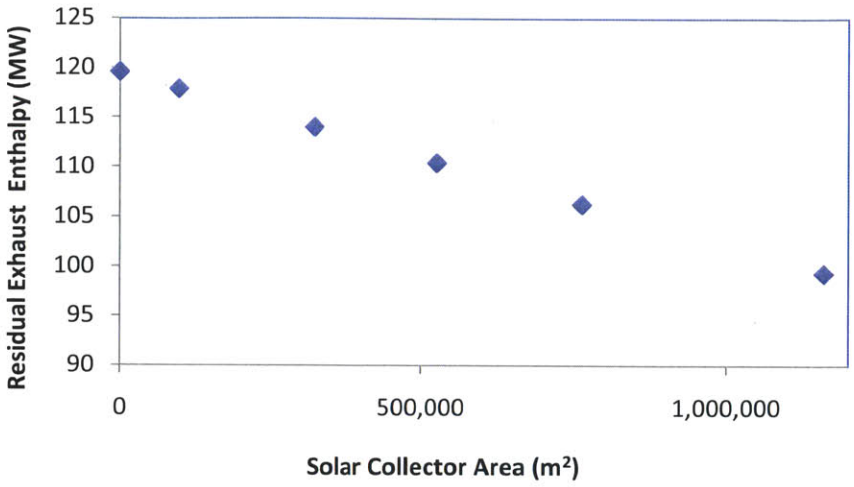

Figure 9. Plot of Residual Exhaust Enthalpy versus Solar Collector Area in Bottoming Cycle of AZEP Hybridized with Solar Vaporizers. The Residual Exhaust Enthalpy is calculated assuming zero reference point of enthalpy at 300K.

To further investigate the apparent insensitivity of incremental solar efficiency to changes in solar share (by increasing total trough length and area of collectors), the solar to heat efficiencies of the parabolic troughs were calculated, shown in the TABLE below:

TABLE 4. Solar to Thermal Efficiency of parabolic troughs with varying total collector area.

Total Collector Area (m^2)	98,000	323,000	526,000	764,000	1,160,000
Solar to Thermal Efficiency (%)	43.23	43.43	43.40	43.48	43.56

As can be seen in **TABLE 4**, the solar to thermal efficiency was not greatly affected by changes in solar share of input. Optical losses are independent of trough length and Therminol temperature. Therefore, the result of **TABLE 4** implies that the fraction of incoming heat that is lost to the atmosphere does not change appreciably. The troughs are set up so that incoming temperature is 317°C for all of the troughs. The exit temperature varies from 322°C to 356°C depending on the total length of the trough. The heat loss in the trough is driven by temperature difference between Therminol and the atmosphere. Furthermore, the change in exit temperature only affects part of the troughs: the temperature profile in the beginning of longer troughs is essentially identical to that of a shorter trough. These factors combined may have led to changes in heat loss not playing a significant role and solar to thermal efficiency remaining more or less constant.

When combining the insights from **Figures 8, 9** and **TABLE 4**, we see that hybridization with an increasing solar share exhibits entropy generation due to temperature mismatch, increased

enthalpy extraction from the exhaust and constant solar to thermal efficiency. These factors combined may explain the results shown in **Figure 7**- seemingly constant incremental solar efficiency.

6. Insolation Dependence of Hybrid Thermodynamic Performance

Solar insolation varies greatly at different times in the day and on different days. Therefore, the response of solar hybrid cycles to changes in insolation is a key factor in the effectiveness of those cycles. This section investigates the effect of variations in the level of insolation on the hybrid's thermodynamic performance.

Simulation Description

For the simulation of the high pressure solar-thermal vaporizer hybridized AZEP cycle with changes in solar insolation, the cycle design was unchanged (**Figure 6**). The only change made was to fix the total collector area vary solar insolation.

The total collector area was chosen to be 550,000 m^2. This is comparable to current parabolic trough fields [19]. The collector area was chosen to correspond to typical solar insolation (**Figure 10**). The pipe length was chosen to be 100,000m, maintaining the same aperture width as previous simulations. The solar insolation was varied and cycle performance metrics calculated. There is an upper limit to possible solar insolation that can be used for vaporization- the scenario when all high pressure steam vaporization is provided by solar energy.

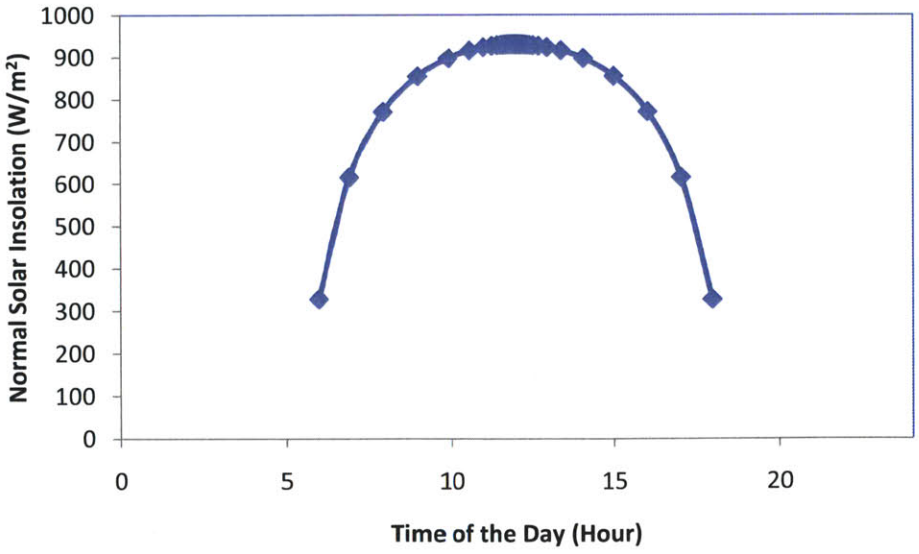

Figure 10. Measured normal solar insolation in Dhahran, Saudi Arabia on June 20 as a function of time of the day.

Simulation Results

The major thermodynamic findings of varying solar insolation are plotted in the figures below.

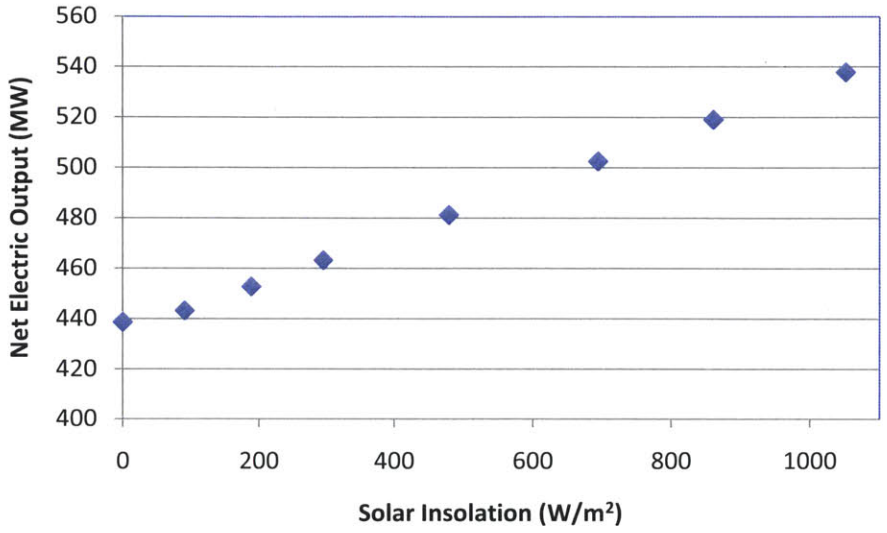

Figure 11. Variation of Net Electricity Produced of Solar Hybridized AZEP with Solar Insolation.

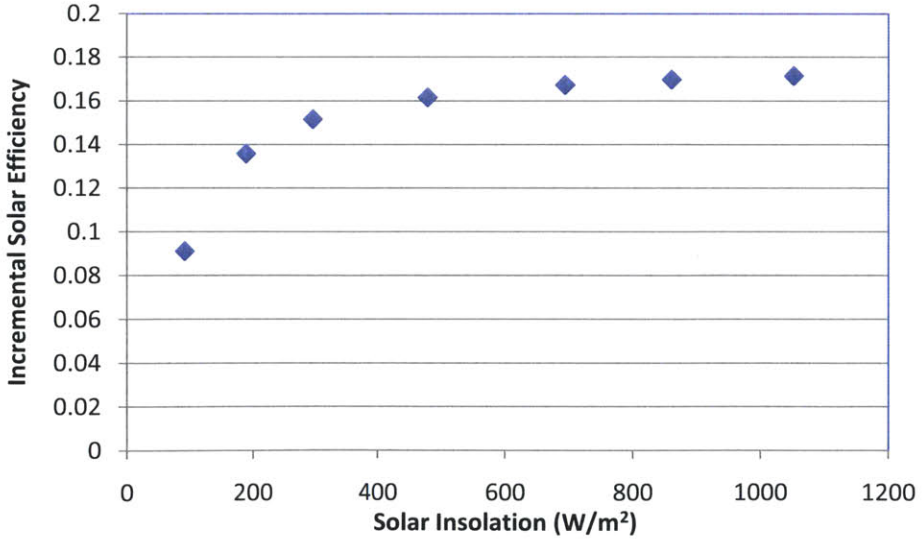

Figure 12. Variation of Incremental Solar Efficiency of Solar Insolation in Solar Hybridized AZEP with Solar Insolation.

As expected, the net electric output increased with increasing solar insolation (**Figure 11**). This indicates that the proposed hybrid power plant reaches peak power production at times

of high insolation. At times of very low insolation the plant effectively acts as a non-hybridized AZEP cycle. From **Figure 12**, we see that incremental solar efficiency increases with solar insolation, reaching a plateau at about 17%. Therefore, as insolation increases, the hybrid has both a higher solar share and a higher efficiency of converting solar energy to electric power. As a consequence, net electric output grows rapidly with solar insolation.

One possible explanation of the source of this increase in incremental solar efficiency lies in the pressure drop in the solar troughs. Given that the length of the parabolic troughs and flow rate of the heat transfer fluid through the troughs is maintained constant, the pressure drop in the troughs is not expected to change appreciably for different levels of insolation. As solar insolation increases, the energetic penalty of this pressure drop becomes a smaller fraction of the incoming solar heat, leading to an increase in incremental solar efficiency. This can be seen in **Figure 13** below, which shows the incremental power out (i.e. net power minus power produced by a non-hybridized reference AZEP with same fuel input) and the power loss due to pressure drop in the parabolic troughs for different levels of solar insolation. It can be seen that as insolation increases the pressure drop becomes less significant.

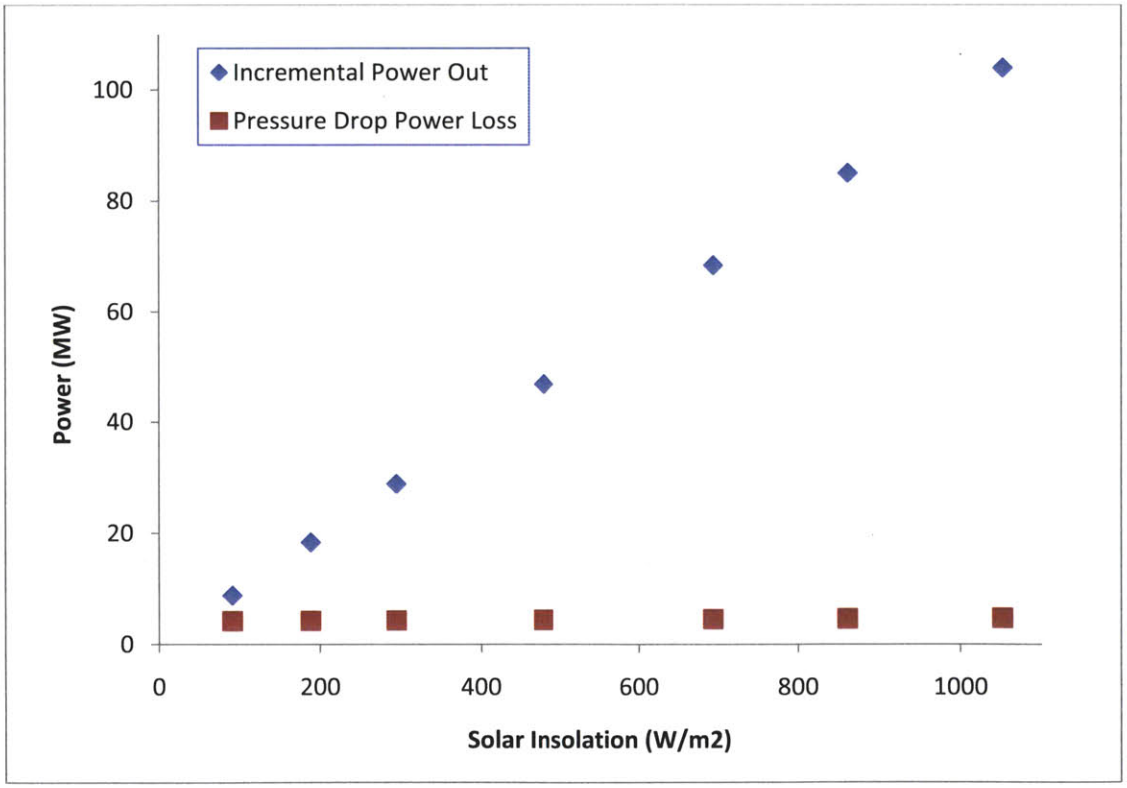

Figure 13. Loss of Power in Parabolic Trough due to Pressure Drop compared to Incremental Solar Power for Different Levels of Solar Insolation

Another source of energy loss in parabolic troughs is heat loss to the surrounding environment. This heat loss is modeled in the parabolic trough as a 1D combination of heat

resistors in series. Heat loss is driven by the temperature difference between the bulk Therminol in the receiver and ambient air. The bulk temperature of Therminol in the receiver pipe is increased from an inlet temperature of 317 °C to a varying outlet temperature depending on the insolation, with the upper limit being 356 °C. Therefore, the value of $T_{bulk} - T_{ambient}$ spans the range of 290°C to 329°C (~13% change). On the other hand, the enthalpy transfer to Therminol is on the order of $T_{out} - T_{in}$, which has a much larger span as insolation changes (from 5°C for insolation of 100W/m^2 to 29°C for insolation of 1050 W/m^2). The total area and length of the troughs is maintained constant, so the only source of difference in heat loss is from changes in T_{bulk}-$T_{ambient}$. Since T_{bulk}-$T_{ambient}$ changes very little compared to the change in insolation, heat loss in the parabolic trough becomes a smaller fraction of total heat received by the trough as insolation increases. This is consistent with an increase in incremental solar efficiency with increasing insolation. Furthermore, this result is not inconsistent with observed dependence of solar efficiency on solar insolation in solar-only plants (**Appendix B**).

In designing the trough field, a relatively high flow rate of Therminol was chosen. The rationale behind this choice and the tradeoffs involved are discussed here. Higher flow rates of Therminol imply that a lower change in temperature is needed to achieve the desired enthalpy rate. Given that Therminol is being used for vaporization, the inlet temperature of the trough cannot be changed, so any reductions in the change in temperature in the trough imply a decrease in the exiting temperature of Therminol. For a constant inlet temperature, decreasing exit temperature decreases heat loss to the environment, which is favorable. Furthermore, decreasing the change in Therminol temperature needed for vaporization means causes better temperature profile match in the heat exchanger, leading to a drop in entropy generation. On the other hand, high flow rates of Therminol, lead to an increase in power loss due to pressure drop in the trough, which is unfavorable. Therefore, there is a tradeoff between heat losses in trough, entropy generation in vaporizer and pressure drop in the trough that needs to be considered when deciding on Therminol flow rates. As shown in **Figure 13**, this tradeoff is most significant at times of low solar insolation.

7. Alternative Design: Solar-Thermal Direct Preheating of High Pressure Water

Alternatively, solar-thermal energy can be used as a source of energy for preheating water prior to vaporization in the bottoming cycle of AZEP. Parabolic troughs are used directly to preheat incoming high pressure water streams to saturation, prior to vaporization. This section presents the simulation results for this hybridization scheme.

Design Description

The AZEP cycle incorporates a heat recovery steam generation system for extracting heat from the exhaust stream and the combustion products to heat and vaporize water streams at three pressure levels. Solar energy can be used to preheat the high pressure water stream prior to vaporization to increase power generation in the bottoming cycle. To investigate this, an ASPEN Plus® model of AZEP was hybridized by the introduction of parabolic troughs to directly heat the high pressure water streams to saturation, as shown in the schematics below (**Figure 14, 15).**

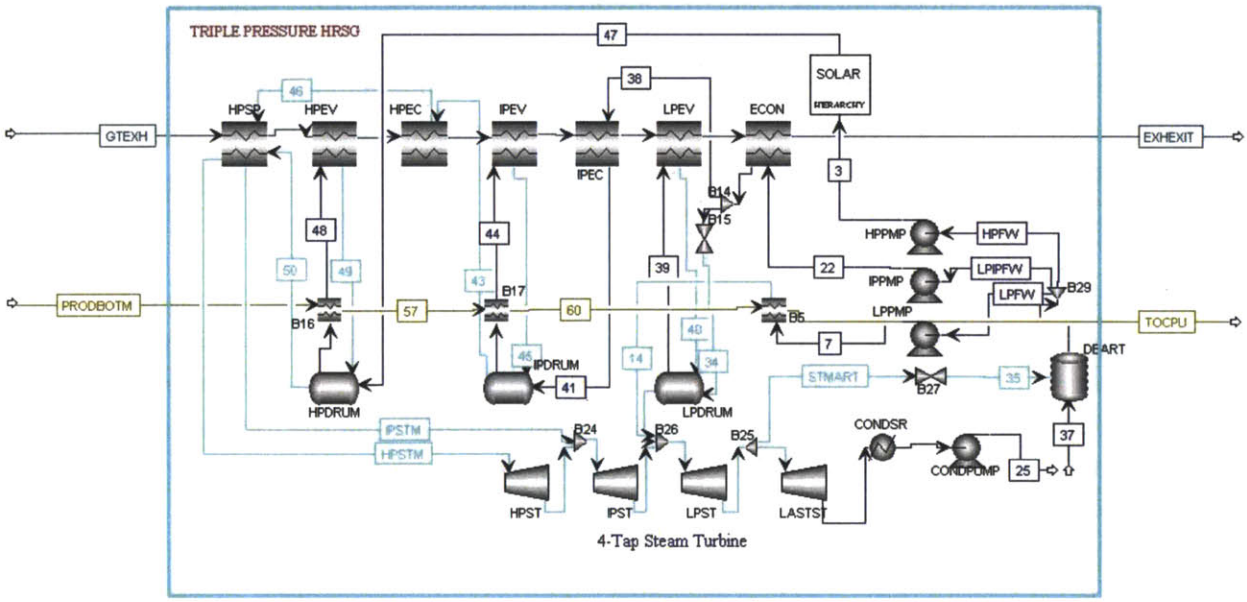

Figure 14. Schematic of AZEP Bottoming Cycle with Direct Solar Preheating of High Pressure Water Stream.

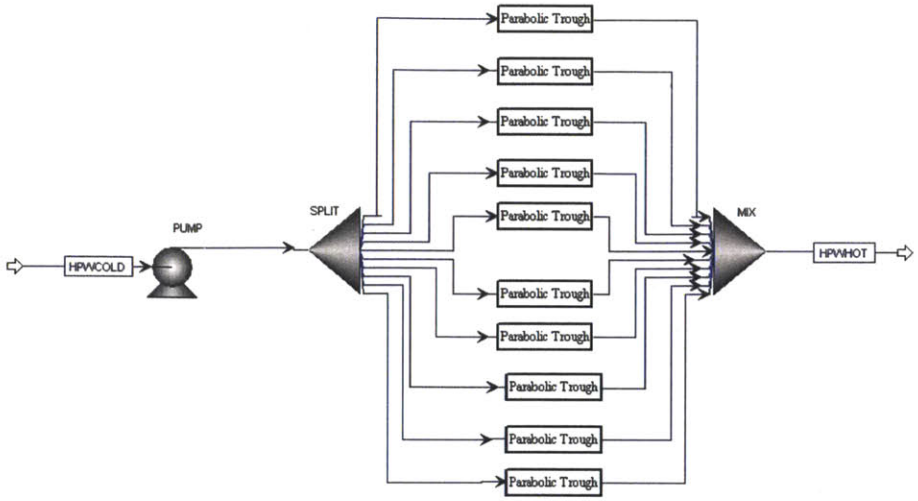

Figure 15. Schematic of Direct Solar Heater Parabolic Trough Setup. Incoming high pressure water is heated by 10 parabolic troughs running in parallel.

Simulation Description

The solar parabolic trough field is composed of 10 parabolic troughs running in parallel to preheat water prior to vaporization. The area and length parameters of the troughs were varied (maintaining the area: length ratio constant) by a design specification in ASPEN Plus® so that the water stream flowing out of the troughs is at liquid saturation. This is a simulation of the solar-hybridized bottoming cycle at an instant in time, so it assumes constant solar insolation and angle of incidence.

The properties and input parameters used for the solar parabolic troughs are shown in the TABLE below.

TABLE 5: Input Parameters and Properties Used in Simulation of Solar Parabolic Troughs for Direct Water Heating.

Number of Parallel Troughs	10
Solar Insolation	500 W/m^2
Incident Angle	45°
Output (HPWHOT) Pressure	100 bar
Output Vaport Fraction	0 (Saturated Liquid)

Simulation Results

This section presents the major findings of the simulation of this hybridization scheme. A summary of the energetic results is presented in **TABLE 6**.

TABLE 6. Result of Simulation of AZEP Plant with Solar-Thermal High Pressure Water Preheating. The energetic parameters for the non-hybridized cycle (light grey) and for a cycle hybridized with the same area of solar troughs through indirect steam vaporization are presented for reference.

	Non-Hybridized	Steam Vaporization	Water Preheating
Area of Solar Troughs (m^2)	N/A	984,000	984,000
Solar Heat Input (MW)	0	492	492
Solar Share of Input (%)	0	35.0	35.0
Net Electricity Produced (MW)	438.7	518.6	**501.3**
First Law Efficiency (%)	47.93	36.84	**35.62**
Second Law Efficiency (%)	46.08	35.97	**34.78**
Solar Share of Output (%)	N/A	16.63	**13.79**
Incremental Solar Efficiency (%)	N/A	16.23	**12.73**

It was found that the addition of solar-thermal water preheating increased Net Electric Power produced from 438.7 MW to 501.3 MW. In comparison, the addition of solar-thermal steam vaporization- at an equal solar share- increased Net Electric Power to 518.6 MW. Consequently, hybridization through water preheating had lower first, second and incremental solar efficiencies.

A potential cause of the relative inefficiency of this hybridization scheme is an increase in temperature profile mismatch. To investigate that effect, the temperature profiles in the heat exchangers between the gas turbine exhaust and water flows is plotted for the three scenarios: non-hybridized, hybridized with steam vaporization and hybridized with water preheating (**Figure 16**).

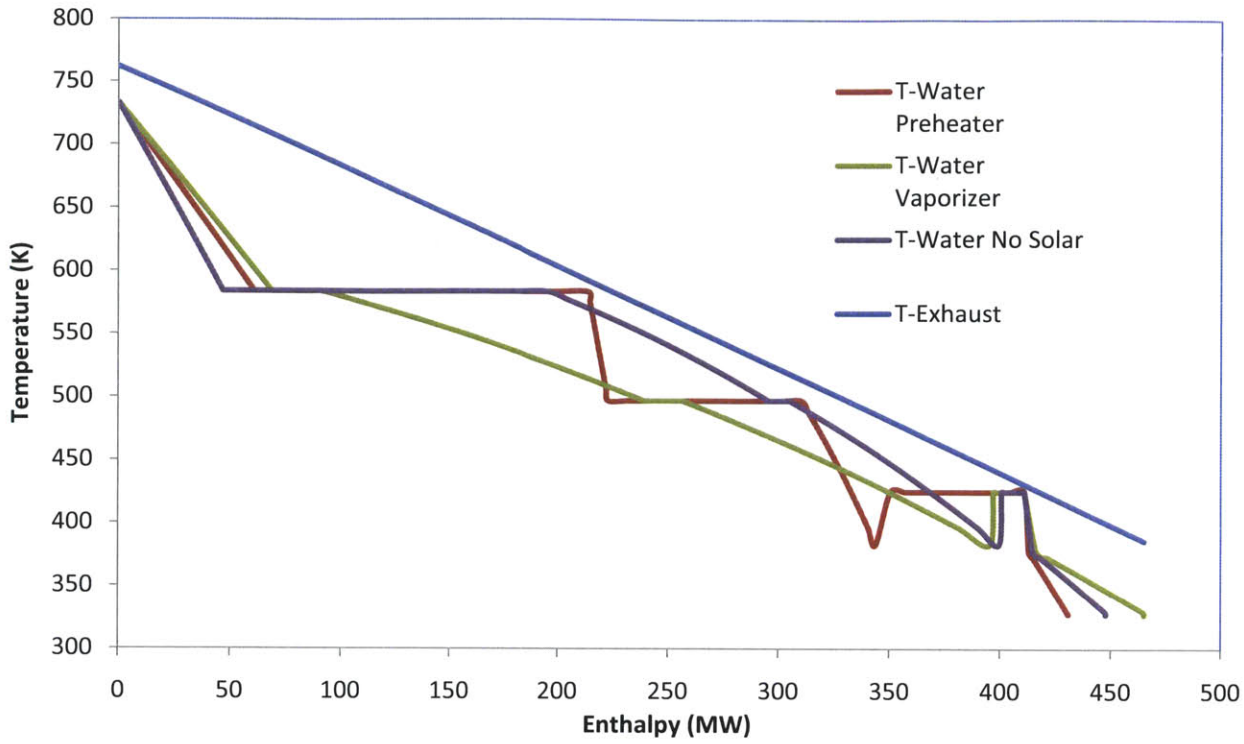

Figure 16. Pinch Diagram for Gas Turbine Exhaust Heat Exchangers in Bottoming Cycle for a non-hybridized AZEP cycle (purple), a high pressure steam solar vaporizer hybridized cycle with solar share 35% (green) and a high pressure water preheater hybridized cycle with solar share 35% (red).

By inspecting the pinch diagram, it can be seen that this proposed hybridization scheme leads to larger vaporization load compared to the two other cycles. Vaporization zones are typically associated with large entropy generation due to temperature mismatch. Specifically, when the preheat hybridization scheme is compared to the non-hybridized cycle, the hybrid appears to have a higher temperature mismatch and hence higher entropy generation. When comparing this scheme to the vaporizer scheme, however, it appears that the temperature profile is better matched in the preheater design. Therefore, temperature profile mismatch does not explain the apparent inefficiency in the preheater hybridization scheme.

The preheater decreases the load needed to heat the water streams at lower temperatures. This may lead to a drop in the enthalpy recovered from the exhaust stream (the exhaust being sent to CCS at a relatively high temperature), which may explain the drop in efficiency. The temperature and residual enthalpy of the exhaust stream leaving the HRSG is tabulated for the three cycles in **TABLE 7**. It can be seen that the exhaust temperature and residual enthalpy are higher in the water preheating hybridized cycle than in the non-hybridized cycle. Therefore, this hybridization scheme extracts less enthalpy from the exhaust, which may explain the relatively low efficiency. In comparison, the steam vaporization hybrid extracts more enthalpy from the exhaust than the non-hybridized cycle. The difference in enthalpy recovery between the two hybridization schemes is large (34.1 MW) and it may account for the difference in net electric power produced (17.3 MW).

TABLE 7. Temperature and Residual Enthalpy of Exhaust Stream Exiting the Bottoming Cycle. The values are presented for three cycles: non-hybridized, hybridized by high pressure steam vaporization with solar share of 35% and hybridized with high pressure water preheating to saturation with solar share of 35%.

	Non-Hybridized	Steam Vaporization	Water Preheating
$T_{exhaust, out}$ (K)	119.61	102.39	136.52
Residual Enthalpy (MW)	400.4	386.0	414.5

8. Thermodynamic Synergy Analysis

In the above sections, the thermodynamic performance of AZEP hybridized with solar thermal parabolic troughs was analyzed. To assess if there are any thermodynamic benefits from hybridization, the coupled plant's thermodynamic performance should be compared to a combination of single energy input plants. In the following section, the performance of the hybrid plant is compared to that of a linear combination of AZEP and best known solar-only parabolic trough plants. In essence, we are assessing whether electric output is higher if the energy inputs are used to produce power separately or in a hybridized plant. This analysis does not take into account economic considerations, it is purely thermodynamic. Note that this analysis can be seen as a special case of the linear combination metric proposed in [5, 20].

Potential thermodynamic advantage from hybridization was estimated by evaluating three quantities:

-The power output of the solar-thermal hybridized AZEP cycle with solar energy used as a heat source for vaporization of high pressure steam.

-The power output of a non-hybridized AZEP cycle (with an equal fuel input to the hybrid).

-The power output of best technology solar-only parabolic trough based power plant (with the same collector area as the hybrid).

For this section, the power output of the hybrid is based on a collector area of 550,000m^2 and a solar insolation of 1000W/m^2. The power output of the AZEP plant is based on the work by Mancini [4]. The power output of a solar-only parabolic trough plant was estimated based on data on the performance of SEGS VI power plant, when operating without fossil-fuel backup [19]. The total receiver area of SEGS VI is 188,000 m^2 (not 550,000 m^2), therefore, the power output was scaled up proportionally (essentially assuming modular scale up). This solar-only power output is based on a solar insolation of 1000W/m^2.

TABLE 8. Synergy Analysis – Comparison of net power output of solar hybridized AZEP cycle with a linear combination of two single energy mode plants: AZEP and SEGS VI.

Plant Type	Net Power Output (MW)
AZEP 100	439
Solar – Only (SEGS VI)	38
Linear Combination	549
Solar - Hybridized AZEP	533
Net Gains From Hybridization	-16

This analysis finds that a linear combination of the two single energy mode power plants is thermodynamically favorable to hybridization, i.e. there are no thermodynamic gains from hybridization.

It is important to note that this analysis is for a particular level of insolation and does not take into account the time dependence of insolation level and incidence angle. There may be thermodynamic advantages that are not captured by this study due to temporal differences in

power production between the hybrid and the SEGS cycle. While peak performance appears to be better in the separate single energy mode plants than the hybridized plant, differences in off-peak performance may render the hybrid thermodynamically favorable. This will be discussed further in the following section.

9. Discussion and Conclusion

An analysis of the performance of an AZEP cycle hybridized with solar parabolic troughs in the HRSG Bottoming Cycle is presented for two configurations: indirect vaporization of high pressure steam and direct heating of high pressure water flow prior to vaporization. Numerical simulations and thermodynamic analysis lead to concluding that the former configuration is more efficient. Thus, a representative hybrid of that configuration is compared to a linear combination of single energy mode plants with equivalent fuel and solar inputs. It is concluded that the hybridization of AZEP with supplementary solar heating in the bottoming cycle, in its current configuration, does not present any thermodynamic synergy. In this section, the reasons behind this observed inefficiency in hybridization are discussed. Additionally, potential benefits of hybridization not captured by the above analysis are discussed, leading into the need for a full cost analysis. Finally, potential improvements to the design and future areas of investigations are suggested.

The above simulations are not optimized; therefore, there may be more efficient configurations. In particular, the flow rates of water in the different pressures may be adjusted to achieve higher efficiencies by improving enthalpy extraction and minimizing exergetic losses due to temperature mismatch. In the case of the solar vaporizer, it may be possible to better match the temperature profile in the heat exchangers by a more optimal configuration of water flow rates, hence, reducing entropy generation in the bottoming cycle and increasing efficiency. Prior to the simulation, it was expected that by reducing the heat load of vaporization temperature mismatch can be decreased. This may still be achieved by re-design or optimization of the steam flows at the 3 different pressure levels. In the case of solar preheating, the simulated hybrid extracted less enthalpy from the exhaust than the non-hybridized cycle. Modifications in the water flow rates may provide more optimal enthalpy extractions and better thermodynamic performance.

Decisions in trough field design have an impact on the efficiency of the parabolic troughs. Inherent tradeoffs in field design imply that there is room for optimization of trough field design parameters. For example, as described in **Chapter 6**, increasing the flow rate of the heat transfer fluid in the solar vaporizers decreases heat loss in troughs and entropy loss in the solar vaporizer but leads to an increase in pressure drop in the trough. Therefore, the choice of flow rate of the heat transfer fluid presents tradeoffs and has room for improved efficiency through optimization.

An important advantage from hybridization that is not captured in the above analysis is that hybrid plants provide dispatchablity without the need for thermal storage. Additionally, these power plants exhibit peak power output during daytime, which is aligned with peak power demand. This temporal alignment of power supply and demand may improve efficiency of power production by reducing losses due to power plants operating at non-optimal outputs due to the variability of demand. A detailed investigation of fluctuations in energy demands by time of the day may be coupled to case studies of this design in future work to assess this claim.

This work is not a case study of a particular site that uses site data on solar insolation and incidence angle in simulations of the cycle. Rather, the work simulates thermodynamic performance at snapshots in time and does not follow the changes in solar insolation and angle of incidence in any given day and over the course of the year. While this work simulates the hybrid

with variable solar insolation, it is only to show the effect of solar insolation on plant performance and it is not sufficient to provide a temporal account of plant output and performance. A case study is necessary for full characterization of the performance of this design.

As shown in **Chapter 5**, the proposed solar vaporizer hybridization scheme can be applied at a wide range of input solar shares. This is important as many cost and logistical considerations will factor in the choice of size of solar field. Furthermore, the analysis in **Chapter 6** showed that the design is flexible to changes in solar insolation, which is critical since solar insolation varies greatly throughout the day and across the year, both due to the position of the sun and changes in weather.

In the absence of thermodynamic benefits from hybridization, there may be economic factors that make hybridization an attractive option. When compared to two separate single energy mode plants, a hybrid may require a lower initial capital cost due to common machinery. Additionally, operation costs are greatly influenced by the economies of scale. Therefore, a cost analysis of this proposed cycle is critical for comparison to alternatives. It is important to note that this hybrid is a zero-emissions cycle, unlike typical solar-fossil fuel hybrids. The solar share does not affect carbon dioxide emissions since both technologies are emissions free. Any cost comparison of this hybrid to alternatives needs to take into account carbon dioxide emissions. Ultimately, an economic analysis should be performed comparing this technology to other zero-emission options. Such an economic analysis should take into account both the cost of power production and the temporal alignment of power output and demand.

The work we presented is a thermodynamic analysis of the proposed hybrids to assess the potential for benefits from hybridization. Further investigations are necessary to completely characterize the suitability of such hybridization. Particularly, the observed inefficiencies may be minimized by optimization of steam flows in the bottoming cycle. Additionally, since the inefficiencies in the two proposed hybridization schemes have different sources, it may be advantageous to look at the performance of a cycle that employs both hybridization schemes. Ideally, a case study of the plant using solar insolation, environmental and energy demand data from a particular site could be performed. Such case study, alongside a cost analysis, is necessary to fully assess the suitability of the proposed plant.

In conclusion, we have proposed designs for a solar hybridized Advanced Zero Emissions Plant, which makes use of solar trough to provide supplemental energy to the bottoming cycle. From thermodynamic analysis, we find that there are no gains from hybridization (synergy). Further analysis of the plant design's annualized performance in a case study and comparison to alternatives is necessary to determine if there are thermodynamic gains from hybridization arising from differences in off-peak performance. Additionally, economic gains from hybridization should be assessed through estimation of cost of electricity produced by the hybrid.

Appendix A

This section is a description of the bottoming cycle simulation as implemented by Mancini [4].

The bottoming cycle is a triple pressure heat recovery stream generation system (**Figure 16**). Heat from the gas turbine exhaust is used in 7 consecutive heat exchangers (HPSP, HPEV, HPEC, IPEV, IPEC, LPEV, ECON) to produce steam. Additionally, heat is extracted from the combustion product to supplement vaporization of the water flow at the three pressures in three separate heat exchangers (B17, B16, B5).

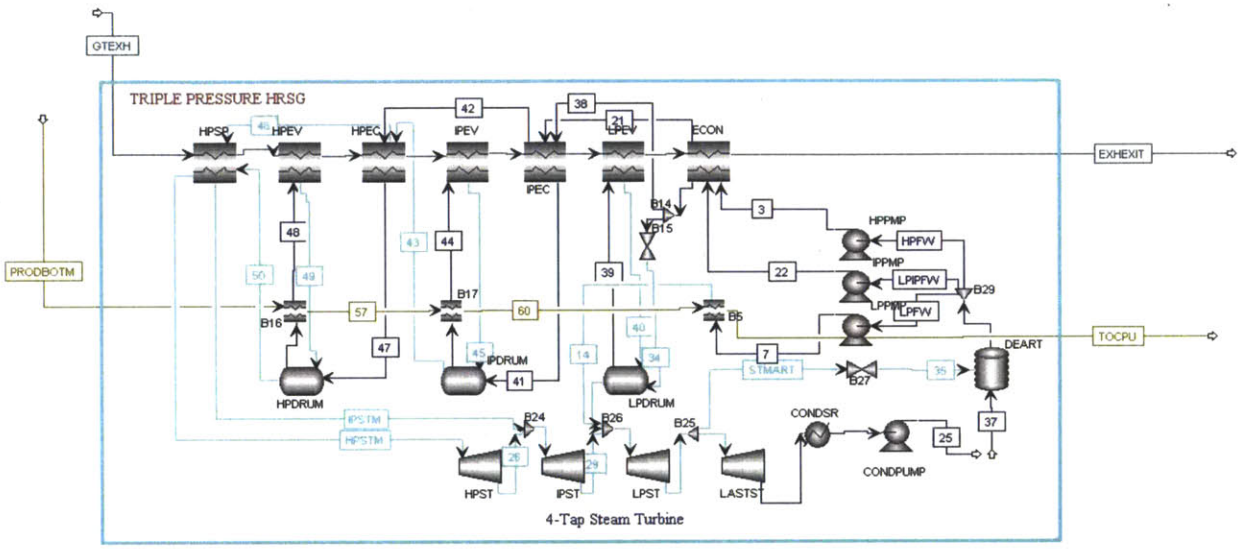

Figure 17. ASPEN Plus® Model - Triple Pressure Heat Recovery Steam Generator

Feedwater is combined with recycle steam in a Deaerator to remove dissolved gases. The feed water is then split into three separate streams, which are pumped to pressure levels: 100bar (HP), 25bar (IP) and 5 bar(LP).

The high pressure stream is heated in the following sequence:

-Heated to 110°C in the economizer (ECON).

-Heated to 224°C in the intermediate pressure economizer (IPEC).

-Heated to a vapor fraction of 0 (T = 311°C) in the high pressure economizer (HPEC).

-Vaporized partially in B16 (with pinch set at 5°C).

-Vaporized to vapor fraction of 1 in the high pressure evaporator (HPEV).

-Superheated to 460°C in the high pressure super-heater (HPSP).

The intermediate pressure stream is heated in the following sequence:

-Heated to 110°C in the economizer (ECON).

-Heated to a vapor fraction of 0 (T = 224°C) in the intermediate pressure economizer (IPEC).

-Vaporized partially in B17 (with pinch set at 4°C).

-Vaporized to vapor fraction of 1 in the intermediate pressure evaporator (IPEV).

-Superheated to 311°C in the high pressure economizer (HPEC).

-Superheated to 460°C in the high pressure super-heater (HPSP).

The low pressure steam comes from two sources. Part of the intermediate pressure stream is adiabatically flashed down to a pressure of 5 bar after heating in ECON. This low pressure stream is then vaporized to vapor fraction of 1in LPEV. The second source of low pressure steam is feedwater that was pumped to 5 bars and then evaporated in B5.

The flow rates in the bottoming cycle are set by two design specs:

- The total feedwater flow is designed for an LPEV pinch of 6°C.
- The low pressure feedwater flow is designed for a B5 pinch of 10°C.

Model assumptions in the cycle design, cycle component can have a significant effect on simulation results; hence, they are presented in the TABLE below.

TABLE 9. ITM-Power Cycle Assumptions. TIT= Turbine Inlet Temperature, PR = Pressure Ratio [Adapted from Mancini]

ITM T(K)/ P(bar)	ITM ΔP Feed/Perm.	Gas Turbine TIT/PR	Turbo-machine GT/COMP η_{II}	ITM-HEX Pinch/ΔP	Steam Turbine η_{II}/TIT
973-1273 /20-10	Calculated	1573/20	90% / 85%	15 / 3 %	90% /623-773

Appendix B

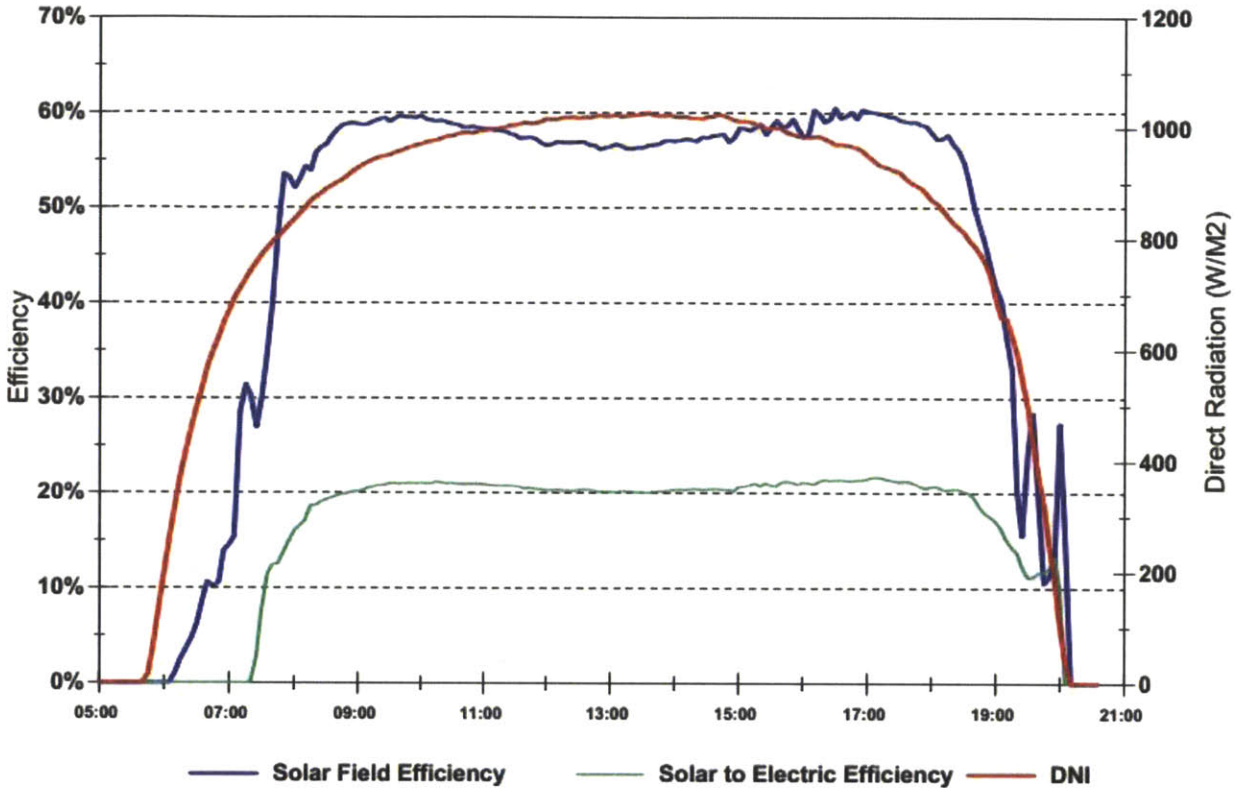

Figure 18. Plot of Solar Radiation, Solar to Electric Efficiency and Solar Field Efficiency as a function of time as measured in SEGS VI [19].

Bibliography

1. T. Barker, I. Bashmakov, L. Bernstein, et al. 2007: Technical Summary. In: Climate Change 2007: Mitigation. Contribution of Working Group III to the Fourth Assessment Report of the Intergovernmental Panel on Climate Change. Cambridge University Press, Cambridge, United Kingdom and New York, NY, USA.

2. International Energy Agency. CO2 emissions from fuel combustion. IEA Statistics, 2009.

3. B. A. van Hassel. Oxygen transfer across composite oxygen transport membranes. Solid State Ionics, 174(1-4):253-260, 2004.

4. N.D. Mancini. Systems-Level Design of Ion Transport Membrane Oxy-Combustion Power Plants. Master Thesis. Massachusetts Institute of Technology. 2011.

5. E. J. Sheu, A. Mitsos, A. A. Eter, E. M. A. Mokheimer, M.A. Habib, and A. Al-Qutub. A Review of Hybrid Solar- Fossil Fuel Power Generation Systems and Performance Metrics. ASME Journal of Solar Energy Engineering. In Press, 2012.

6. E. A. DeMeo, and J.F. Galdo. Renewable energy technology characterizations. Tech. rep., Electric Power Research Institute (EPRI) and U.S. Department of Energy. 1997

7. S. Oda, and H. Hashem. A case study for three combined cycles of a solar-conventional power generation unit. Solar & Wind Technology, 5, pp. 263–270. 1988

8. B.F. Moeller, T. Torisson and M. Assadi. AZEP Gas Turbine Combined Cycle Power Plants - Thermo-economic Analysis. Int J of Thermodynamics 9(1):21-28, 2006.

9. J. M. Amann, M. Kanniche, and C. Bouallou. Natural gas combined cycle power plant modified into an O2/CO2 cycle for CO2 capture. Energy Conversion and Management, 50(3):510 - 521, 2009

10. A. Darde, R. Prabhakar, J. P. Tranier, and N. Perrin. Air Separation and flue gas compression and purification units for oxy-coal combustion systems. Energy Procedia, 1(1):527 – 534, 2009.

11. E. Kakaras, A. Koumanakos, A. Doukelis, D. Giannakopoulos, and I. Vorrias. Oxyfuel boiler design in a lignite-red power plant. Fuel, 86(14):2144 - 2150, 2007.

12. P. J. Gellings and H. M. Bouwmeester. The CRC handbook of solid state electrochemistry, chapter 14, pages 16-30. CRC press, 1997.

13. Air Products. http://www.airproducts.com/~/media/Downloads/Article/Literature_Cryogenic-Air-Separation-ITM-28007017GLB.ashx , Accessed: 04/17/2012.

14. H. Kvamsdal, K. Jordal, and O. Bolland. A quantitative comparison of gas turbine cycles with CO2 capture. Energy, 32(1):10 - 24, 2007.

15. S. Sundkvist, S. Julsrud, B. Vigeland, et al. Development and testing of AZEP reactor components. International Journal of Greenhouse Gas Control, 1(2):180 - 187, 2007.

16. N. D. Mancini and A. Mitsos. Ion transport membrane reactors for oxycombustion - Part I: Intermediate fidelity modeling. Energy 36(8):4701 - 4720, 2011.

17. N. D. Mancini and A. Mitsos. Ion transport membrane reactors for oxycombustion - Part II: Analysis and comparison of alternatives. Energy 36(8):4721 - 4739, 2011.

18. R. Forristall. Heat Transfer Analysis and Modeling of a Parabolic Trough Solar Receiver Implemented in Engineering Equation Solver. NREL Technical Report, 2003.

19. R. Cable. Solar Trough Generation – The California Experience. ASES Forum. Washington DC. 2001.

20. N. D. Mancini and A. Mitsos. Conceptual Design and Analysis of ITM Oxy-combustion Power Cycles. Physical Chemistry Chemical Physics 13(48): 21351-21361, 2011.